Metabolic changes in reticuloendothelial system following Tisagenlecleucel chimeric antigen receptor T cell (CAR-T) therapy using ^{18}F-FDG PET/CT

Shashi B. Singh[1] MBBS, Om H. Gandhi[1] MS, Cameron Haghshenas[1] BS, Bimash B. Shrestha[1] MBBS, Malia Ahmed[1] BS Jaskeerat Gujral[1] MSE, Saira Khan Niazi[1] MBBS Kishor Khanal[2] MD, Rajshree Singh[3] MD, Niloofaralsadat Motamedi[1] MD, Miraziz Ismoilov[1] MD, Cyrus Ayubcha[4,5] PhD, Sahith Valluru[1] MBBS, Navpreet Khurana[1] MBBS, Patrick Glennan[1] BA, Vanessa Shehu[1] BA, Thomas J. Werner[1] MSE, Mona-Elisabeth Revheim[6,7] MD, PhD, MHA Abass Alavi[1] MD

1. Department of Radiology, Hospital of the University of Pennsylvania, 3400 Spruce St, Philadelphia, PA 19104, USA,
2. Knight Cardiovascular Institute, Oregon Health & Sciences University, 3181 SW Sam Jackson Park Rd, Portland, OR 97239, USA,
3. Mercy Catholic Medical Center, Darby, PA 19023, USA,
4. Harvard Medical School, Boston, Massachusetts, USA,
5. Department of Epidemiology, Harvard T.H. Chan School of Public Health, Boston, MA, USA,
6. The Intervention Center, Division for Technology and Innovation, Oslo University Hospital, 0424 Oslo, Norway,
7. Institute of Clinical Medicine, Faculty of Medicine, University of Oslo, 0313 Oslo, Norway

Keywords: Chimeric antigen receptor T cell (CAR-T) - Tisagenlecleucel - Diffuse large B-cell lymphoma (DLBCL) - Non-Hodgkin lymphoma (NHL) - PET/CT - ^{18}F-FDG

Corresponding author:
Mona-Elisabeth Revheim MD, PhD, MHA, Institute of Clinical Medicine, University of Oslo, Postbox 1078, Blindern, 0316 Oslo, Norway; The Intervention Center, Rikshospitalet, Post box 4950 Nydalen, 0424 Oslo, Norway.
m.e.rootwelt-revheim@medisin.uio.no; mona.elisabeth.revheim@ous-hf.no

Received:
30 November 2025
Accepted revised:
23 March 2026

Abstract

Objective: To evaluate changes in metabolic activity in lymphoma adenopathy and other reticuloendothelial organs–bone marrow, spleen, and liver, in patients with diffuse large B-cell lymphoma (DLBCL) following Tisagenlecleucel therapy, using fluorine-18-fluorodeoxyglucse (^{18}F-FDG) positron emission tomography/computed tomography (PET/CT). **Materials and Methods:** Fluorine-18-FDG-PET/CT scans from 41 DLBCL patients (25 males, 16 females; age: 59.15±13.78, range: 29-81 years) treated with Tisagenlecleucel were retrospectively analyzed. Metabolic activity was quantified in lymphoma adenopathy, bone marrow, spleen, and liver at baseline and post-treatment, with a mean interval of 121.2±63.9 days (range: 35-437 days) between scans. The partial volume-corrected total lesion glycolysis (pvcTLG) and total metabolic tumor volume (TMTV) for lymphoma adenopathy, and average mean standardized uptake value (SUVmean) for bone marrow before and after treatment, were compared using the Wilcoxon signed-rank test, whereas the average SUVmean of spleen and liver was compared using a two-tailed paired t-test. **Results:** Fluorine-18-FDG PET/CT showed significant reductions in metabolic activity of lymphoma adenopathy, bone marrow, and spleen after treatment. For lymphoma adenopathy, pvcTLG decreased from 539.22±831.00 to 491.27±1068.35 (P<0.001), with reduction observed in 80.5% of patients, and TMTV decreased from 46.06± 63.07 to 30.40±41.62 (P<0.001). Mean SUV of bone marrow and spleen decreased significantly from 1.31± 0.37 to 1.16±0.33 (P=0.002), and from 1.96±0.68 to 1.77±0.45 (P=0.017), respectively. However, hepatic SUVmean showed no statistically significant changes from 2.30±0.42 to 2.31±0.40 (P=0.21). **Conclusion:** Fluorine-18-FDG PET/CT demonstrated a decrease in metabolic activity of lymphoma adenopathy, bone marrow, and spleen, after Tisagenlecleucel therapy. However, changes in the liver were not statistically significant. These findings suggest that Tisagenlecleucel chimeric antigen receptor T cell (CAR-T) therapy induces a broad systemic metabolic response within the reticuloendothelial system.

Hell J Nucl Med 2026; 29(1): 2-9 *Epub ahead of print: 7 April 2026* *Published online: 30 April 2026*

Introduction

Tisagenlecleucel, a CD19-directed chimeric antigen receptor T (CAR-T) cell therapy, has demonstrated encouraging results in treating refractory diffuse large B-cell lymphoma (DLBCL), a common subtype of non-Hodgkin lymphoma (NHL) [1]. This autologous therapy employs T-cells genetically engineered to express a CAR construct containing a single-chain variable fragment targeting CD19, a transmembrane protein highly expressed on B cells. The construct includes a 4-1BB co-stimulatory domain that enhances T-cell persistence and anti-tumor activity [2]. The pivotal JULIET trial and subsequent real-world studies have established Tisagenlecleucel as a standard care option for patients with aggressive B-cell lymphomas who have failed two or more lines of systemic therapy [1].

Fluorine-18-fluorodeoxyglucose (^{18}F-FDG) positron emission tomography (PET)/computed tomography (CT) imaging has been widely used for disease staging, restaging, and therapeutic monitoring in patients with lymphoma [3-5]. Fluorine-18-FDG PET/CT has demonstrated utility in quantitatively assessing treatment response following Tisagenlecleucel therapy by evaluating changes in tumor burden pre- and post-therapy using standardized metabolic imaging metrics [5]. However, metabolic changes due to CAR-T cell therapy may occur not only in lymphoma-involved lymph nodes (lymphoma adenopathy) but also in other reticuloendothelial organs, such as the bone marrow, spleen, and liver, following CAR-T cell therapy [6-8]. The changes in metabolic activity within these organs following Tisagenlecleucel therapy remain understudied. This study aims to evaluate changes in metabolic activity in both lymphoma adenopathy and other reticuloendothelial organs, such as the bone marrow, spleen, and liver, following Tisagenlecleucel therapy, in patients with DLBCL, using ^{18}F-FDG-PET/CT.

Materials and Methods

Study subjects

This retrospective study analyzed ^{18}F-FDG PET/CT scans from 41 DLBCL patients (25 males, 16 females; mean age: 59.15± 13.78 years, range: 29-81 years) who underwent Tisagenlecleucel therapy for relapsed or refractory disease between 2018 and 2024 at the Hospital of the University of Pennsylvania (Table 1). For each patient, we evaluated baseline scans obtained prior to initiation of therapy and the first follow-up scans after infusion, with intervals averaging 121.2±63.9 days (range: 35-437 days). This study was approved by the Institutional Review Board and conducted in accordance with the ethical guidelines of the institutional clinical research committee. Informed consent was waived by the IRB due to the retrospective nature of the study.

^{18}F-FDG PET/CT imaging protocol

Positron emission tomography/CT scans were performed 60 minutes after intravenous administration of ^{18}F-FDG (4MBq/kg) in patients with serum glucose levels below 200mg/dL. Images were acquired from the base of the skull to mid-thigh using a 16-detector row LYSO PET/CT scanner with time-of-flight (Gemini TF; Philips Healthcare, Bothell, WA), with 3-minute bed positions. Image reconstruction employed a list-mode maximum-likelihood expectation-maximizing algorithm with 33 ordered subsets and three iterations. Positron emission tomography images underwent attenuation correction using low-dose CT images, as well as corrections for random coincidences and scatter.

Image analysis

This study assessed global metabolic disease activity by calculating partial volume-corrected total lesion glycolysis (pvc-TLG) in diseased lymph nodes, both before and after treatment. We also measured the average mean standardized uptake value (SUVmean) of bone marrow, spleen, and liver to assess changes due to tisagenlecleucel therapy. Lymph node analysis was performed primarily using ROVER software (ABX GmbH, Radeberg, Germany) for PET image quantification, while OsiriX MD software v. 12.5.2 (Pixmeo SARL, Bernex, Sweden) was used as needed to confirm anatomical details on ^{18}F-FDG PET/CT images (Figure 1a). ROVER's segmentation algorithm delineated metabolically active lesions, generating PET parameters such as pvcTLG and total metabolic tumor volume (TMTV). This comprehensive approach accounts for potential underestimation in smaller or heterogeneous lesions, providing a more accurate representation of the total lymphoma burden by combining volumetric and partial volume-corrected metrics with traditional measurements.

For assessment of other organs, we used OsiriX software on fused ^{18}F-FDG PET/CT images. For bone marrow, we employed an iterative thresholding algorithm that delineated continuous regions based on Hounsfield units (HU) (1500HU upper bound, 150HU lower bound) to segment the entire skeleton, enabling quantification of global bone marrow ^{18}F-FDG uptake (Figure 1b and 1c). For the spleen, CT-based regions of interest (ROI) were manually drawn on fused ^{18}F-FDG PET/CT coronal sections to measure average SUVmean for global splenic uptake at baseline and post-CAR-T infusion (Figure 1d). A similar manual approach was used for liver assessment to measure global average SUVmean, carefully excluding bile duct, portal vein, and gallbladder (Figure 1e).

Response evaluation

Response assessment in our patient population was based on the Lugano criteria (JCO 2014), which utilizes the Deauville five-point scale for ^{18}F-FDG PET/CT interpretation. This scale is scored relative to reference activity in the mediastinal blood pool and liver. A score of 1 means no uptake or no residual uptake. A score of 2 means uptake less than or equal to the mediastinum. A score of 3 means uptake greater than the mediastinum but less than or equal to the liver. A score of 4 means uptake is moderately higher than in the liver. Finally, a score of 5 means markedly increased uptake or the presence of new ^{18}F-FDG-avid lesions.

These scores were then translated into response categories, where complete metabolic response (CMR) was defined as a score of 1 - 3 in nodal or extranodal sites with or without a residual mass. Partial metabolic response (PMR) was defined as a score of 4 or 5 with decreased uptake compared to baseline and residual masses of any size. Stable disease (SD) was defined as a score of 4 or 5 with no significant change in uptake. Finally, progressive disease (PD) was defined as a score of 4 or 5 with increased uptake compared to baseline and or new sites of ^{18}F-FDG uptake consistent with lymphoma.

Statistical analysis

The pvcTLG and TMTV for lymph nodes and global SUVmean for bone marrow before and after the initiation of treatment were compared using the Wilcoxon signed-rank test. For the spleen and hepatic assessment, the average SUVmean before and after initiation of treatment was compared using a two-tailed paired t-test.

Results

The characteristics, response parameters, and complications of the involved subjects are summarized in Tables 1, 2, and 3, respectively.

^{18}F-FDG PET/CT image analysis results of various structures

Changes in lymphoma adenopathy

The average pvcTLG before and after treatment were 539.22±831.00 (range: 5.20 to 3194.50) and 491.27±1068.35 (range: 9.80 to 4671.10), respectively. pvcTLG decreased after CAR-T therapy in 33 (80.5%) cases and increased in 8 (19.5%) patients. This difference was statistically significant ($P<0.001$) (Figures 2 and 3). The average TMTV before treatment was 46.06±63.07 (range: 0.80 to 262.70) and after treatment was 30.40±41.62 (range: 1.10 to 159.10), demonstrating an average percent change of -40% between the groups. This difference was statistically significant ($P<0.001$).

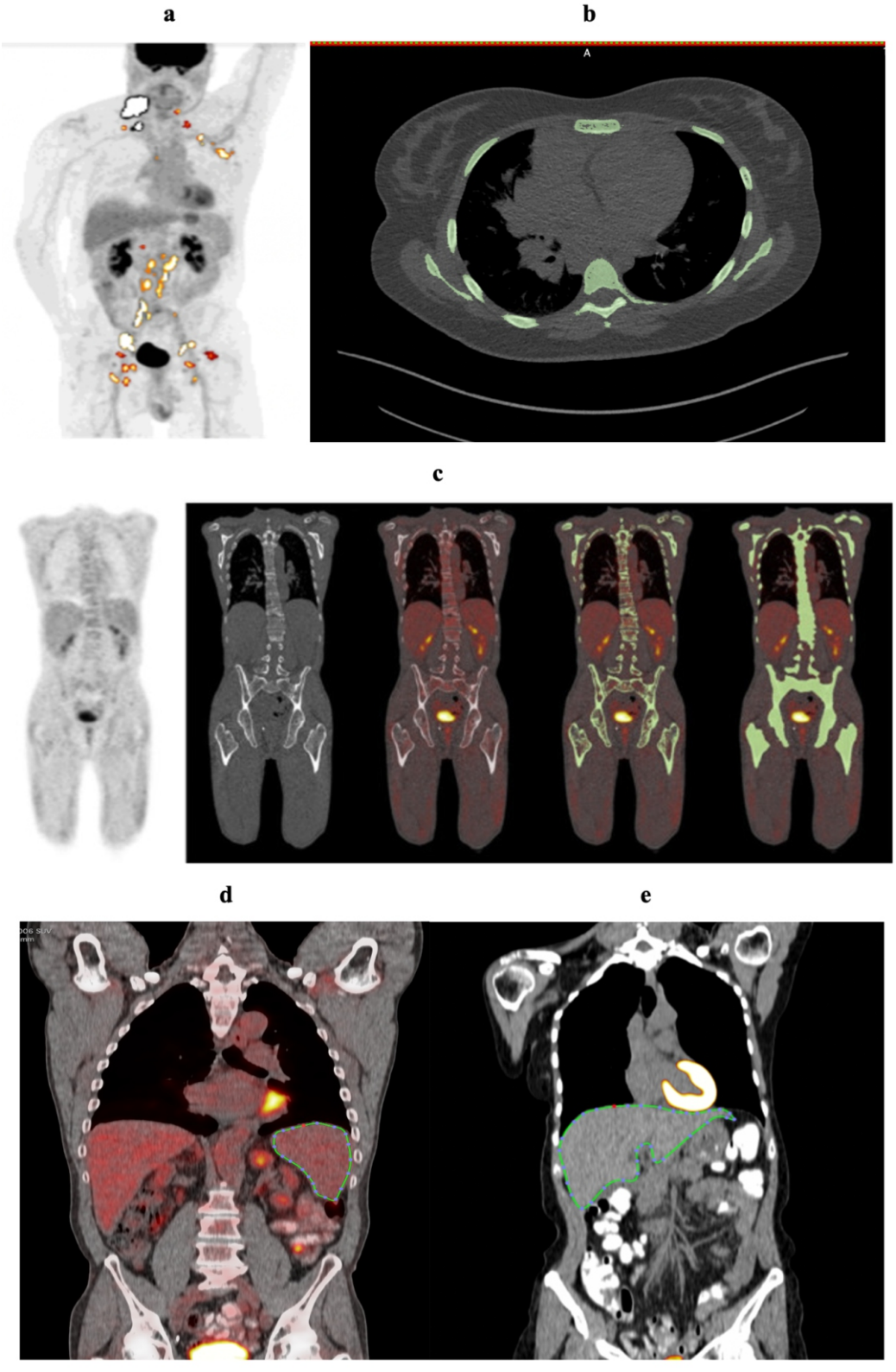

Figure 1. Segmentation method of structures analysed in this study. a) Lymph node active lesions were covered with spherical or cylindrical masks, and lesion boundaries were defined using ROVER software's adaptive thresholding technique with a threshold of 40% of the SUVmax. ROVER software automatically computed pvcTLG, a measure of global lymphoma burden in lymph nodes. b) The fused ^{18}F-FDG PET/CT image shows the method used to assess bone marrow disease, with green color covering the entire bone marrow, indicating the assigned ROI. This segmentation method was performed for all skeletal structures on the PET/CT scan. c) ^{18}F-FDG PET/CT, and fused ^{18}F-FDG PET/CT images demonstrate CT-based segmentation of bone marrow activity using an iterative Hounsfield unit threshold followed by a morphological closing algorithm. The global SUVmean of bone marrow activity was calculated as the average SUVmean of all voxels within the ROI. d) A fused ^{18}F-FDG PET/CT image shows a manually drawn ROI over the spleen in the coronal section. The entire spleen was similarly segmented using Osirix software to calculate the global splenic SUVmean. e) A fused ^{18}F-FDG PET/CT scan displays the hepatic ROI, where the entire liver was segmented while carefully excluding the bile duct, portal vein, and gallbladder.

Table 1. *Characteristics: A summary of demographic and clinical characteristics of the subjects included in this study.*

		Total (N=41)
Age		59.2±13.8 years
Race	White	40
	Asian	1
Gender	Male	25
	Female	16
Final lymphoma diagnosis	Diffuse large B-cell lymphoma (DLBCL)	41
Chemotherapy and immunotherapy	Ibrutinib	2
	Bendamustine	7
	Fludarabine/Cyclophosphamide	2
	None	30
Timeline	# of days between first infusion of CAR-T therapy and interim scan	Average interval of 77.59±29.89 (range: 26-179)
	# of days between baseline scan and first CAR-T therapy infusion	Average interval of 43.56±53.98 (range: 3-332)
	# of days between baseline and interim scan	Average interval of 121.15±63.89 days (range: 35-437 days)

Data expressed as mean±standard deviation or numbers.

Table 2. *Response parameters: A summary of ^{18}F-FDG PET and response parameters for the subjects included in this study.*

		Total (N=41)
Response based on Lugano imaging criteria	Complete metabolic response	24
	Partial metabolic response	7
	Progressive metabolic disease	9
	Incompletely evaluated	1
Average pre-treatment pvcTLG	Lymphoma adenopathy	539.22±831.00 (range: 5.20 to 3194.50)

(Continued)

Average pre-treatment TMTV	Lymphoma adenopathy	46.06±63.07 (range: 0.80 to 262.70)
Average pre-treatment SUVmean	Bone marrow	1.31±0.37 (range: 0.84 to 2.39)
	Spleen	1.96±0.68 (range: 1.32 to 4.37)
	Liver	2.30±0.42 (range: 1.65 to 3.52)
Average post-treatment pvcTLG	Lymphoma adenopathy	491.27±1068.35 (range: 9.80 to 4671.10)
Average post-treatment TMTV	Lymphoma adenopathy	30.40±41.62 (range: 1.10 to 159.10)
Average post-treatment SUVmean	Bone marrow	1.16±0.33 (range: 0.82 to 2.83)
	Spleen	1.77±0.45 (range: 0.87 to 3.28)
	Liver	2.31±0.40 (range: 1.37 to 3.24)

Data expressed as mean±standard deviation or numbers.

***Table 3**. Complications: A summary of treatment complications subjects included in this study experienced.*

		Total (N=41)
Complications	Cytokine release syndrome (CRS)	19
	Neurotoxicity/Immune effector cell associated neurotoxicity (ICANS)	1
	Cytopenias	1
	Atrial fibrillation	0
	Infection (Methicillin-resistant Staphylococcus aureus (MRSA) bacteremia/L3-L4 spine osteomyelitis, pneumonia, and shingles)	1
	Acute exacerbation of congestive heart failure (CHF)	1
	Non-specific (Fever, fatigue, muscle cramps, headache, cough, nausea, vomiting, and upper respiratory symptoms)	9
	None	9

Data expressed as mean±standard deviation

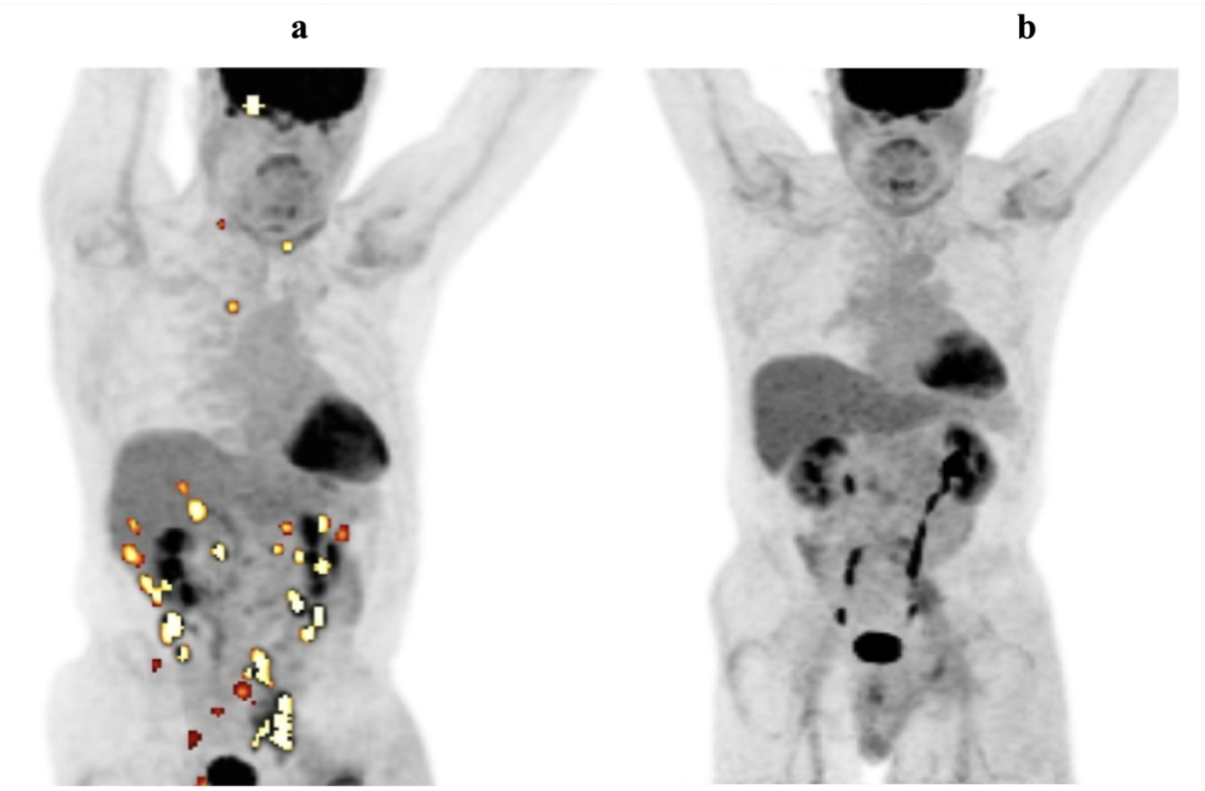

Figure 2. A 68-year-old male patient with diffuse large B-cell lymphoma had a baseline pvcTLG of 273611.3 (a), and 79 days after treatment with Tisagenlecleucel (Kymriah), his pvcTLG decreased to 0 (b).

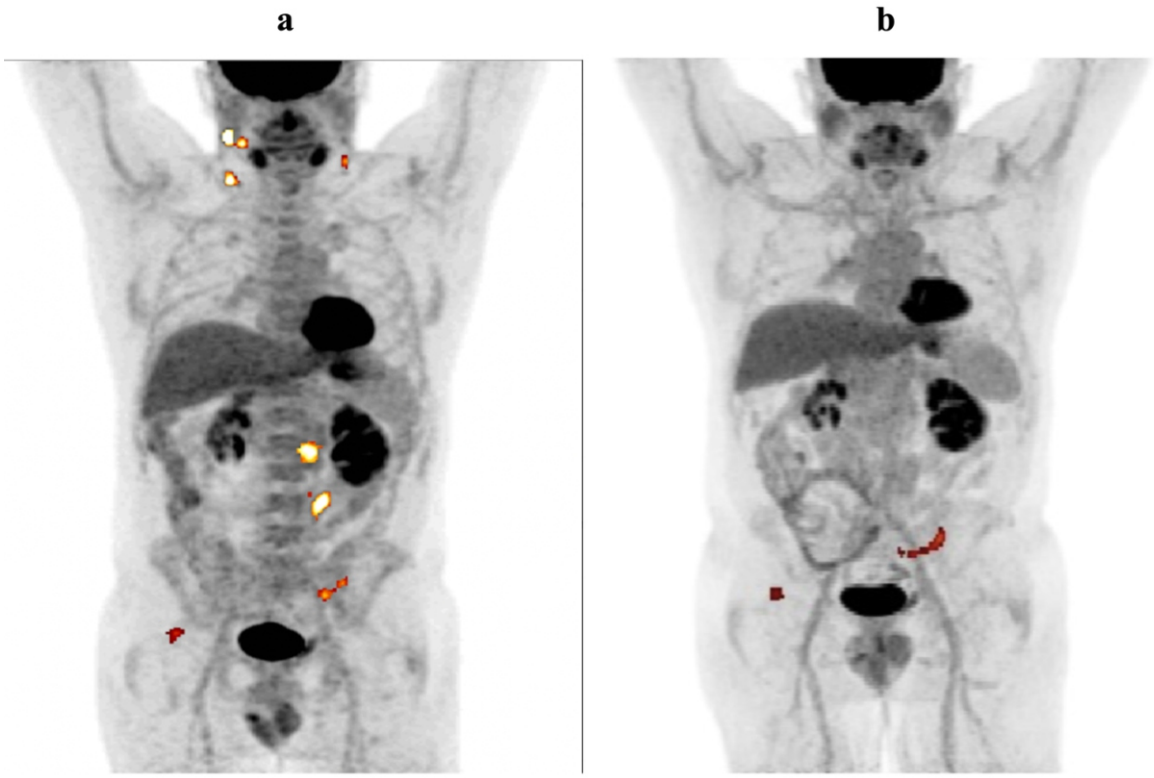

Figure 3. A 55-year-old male patient with diffuse large B-cell lymphoma had a baseline pvcTLG of 2540.8 (a), and 137 days after treatment with Tisagenlecleucel (Kymriah), the pvcTLG decreased to 171.8 (b).

Changes in bone marrow

The global SUVmean before treatment was 1.31±0.37 (range: 0.84 to 2.39), whereas after treatment, it was 1.16±0.33 (range: 0.82 to 2.83), demonstrating an average percent change of -11.45%. Fluorine-18-FDG uptake in the bone marrow decreased after initiation of treatment in 30 (73.2%) and increased in 11 (26.8%) of the 41 cases. This difference was statistically significant (P=0.002).

Changes in spleen

The average SUVmean of the spleen before treatment was 1.96±0.68 (range: 1.32 to 4.37) compared to 1.77±0.45 (range: 0.87 to 3.28) after treatment. The mean difference between the post-treatment and pre-treatment global SUVmean was 0.22±0.66 (range: -3.17 to 0.65). The global splenic SUVmean decreased after initiation of treatment in 25 (61%) and increased in 16 (39%) of 41 cases (P=0.017).

Changes in liver

The global hepatic SUVmean before treatment was 2.30± 0.42 (range: 1.65 to 3.52) compared to 2.31±0.40 (range: 1.37 to 3.24) after treatment. Fluorine-18-FDG uptake in the liver decreased after initiation of treatment in 19 (46.3%) and increased in 22 (53.65%) of the 41 cases. This difference was not statistically significant (P=0.21).

Discussion

This study evaluated the role of ^{18}F-FDG PET/CT using a global assessment technique to characterize changes in metabolic activity in lymphoma adenopathy and other reticuloendothelial organs following tisagenlecleucel therapy in patients with DLBCL. Our findings revealed significant decreases in post-treatment ^{18}F-FDG uptake in lymphoma adenopathy, bone marrow, and spleen following therapy, while uptake in the liver remained statistically unchanged from baseline. These results provide valuable insight into the metabolic response patterns across multiple reticuloendothelial organs in patients receiving this therapy. To our knowledge, this is the first study to comprehensively evaluate changes in the metabolic activity of lymphoma adenopathy and other reticuloendothelial organs, such as the bone marrow, spleen, and liver, following CAR-T therapy using ^{18}F-FDG PET/CT.

Lymphoma adenopathy assessment revealed a significant reduction in pvcTLG and TMTV following tisagenlecleucel therapy. This decline may indicate a metabolic response and potential tumor regression following therapy. This finding aligns with other studies [7, 9, 10]. Derlin et al. (2021) found that achieving remission required early metabolic response (P=0.0476) and that early metabolic changes in lymphoma lesions parallel medium-term response to CAR-T therapy [7]. The difference between our findings and those of Derlin et al. (2021) is that their study focused on early changes at 30- and 90-day post-therapy, whereas our study examined changes at an average of 121 days, capturing longer-term metabolic responses. Georgi et al. (2023) found that 42% of all patients with a complete metabolic response remained in remission 1 year after CAR-T therapy, while a higher total metabolic tumor volume before CAR-T cell infusion was associated with lower chances of a complete metabolic response [9]. The difference between our findings and Georgi et al. (2023) is that their study used axicabtagene ciloleucel in addition to tisagenlecleucel, whereas our study focused on Tisagenlecleucel alone [9].

We found a statistically significant decrease in the global SUVmean of bone marrow after Tisagenlecleucel therapy. While our study focused on changes in SUVmean due to tisagenlecleucel, a similar decrease in SUVmax of the bone marrow has been reported following chemotherapy. Alobthani et al. found a significant reduction from pre-chemotherapy to post-chemotherapy SUVmax of ^{18}F-FDG in the lumbar bone marrow. This may suggest that CAR-T agents such as tisagenlecleucel exert similar effects to those of chemotherapy on the bone marrow [11]. Kenkel et al. (2023) found that bone marrow aplasia could also be a side effect of Tisagenlecleucel, but the mechanism is unclear whether this stems from a reduction or dysfunction of bone marrow or suppression of hematopoietic stem cells [12]. On histological examination, Yeung et al. (2024) found reductions in bone marrow cellularity in 25.5% of patients, approximately 35.5 days after Tisagenlecleucel therapy [13].

We found a statistically significant decrease in the SUVmean of the spleen after therapy. While the decrease in SUVmean of spleen in patients with DLBCL with splenic involvement may indicate a treatment response, the decrease in SUVmean of spleen in those without splenic involvement may suggest a lack of immune response [7]. While assessing splenic metabolic activity as an off-target lymphoid organ due to CD19-targeting CAR-T-cell therapy in DLBCL, Derlin et al. (2021) found that early suppression of metabolic activity in lymphoid organs such as the spleen was associated with a poor outcome [7]. This may suggest that decreased splenic activity may indicate inadequate immune activation rather than treatment success. The spleen serves as a crucial reticuloendothelial organ in both innate and adaptive immune responses, where dendritic cells and T cells interact to facilitate antigen processing and become exposed to proinflammatory cytokines. During immune activation, these cells shift to aerobic glycolysis, which can be detected as increased ^{18}F-FDG uptake. The difference between our findings and Derlin et al. (2021) is the timing of assessment - their study examined early changes (30 and 90 days) associated with poor outcomes [7], while our study evaluated longer-term changes (average 121 days), where decreased splenic uptake may reflect successful resolution of therapy-related immune activation and disease-related inflammation.

We found no statistically significant change in the SUVmean of the liver after tisagenlecleucel therapy. This finding aligns with the established principle that hepatic metabolism remains stable and serves as a reference tissue while monitoring treatment response in lymphoma. Several studies have demonstrated that liver SUVmean is generally stable over time, forming the basis for the Lugano criteria [14-16]. At the same time, some cancer treatments can alter hepatic metabolism [17, 18]. For example, chemotherapy leads to cycle-dependent fatty liver changes in lymphoma patients, and various biological factors, such as body mass index, glucose levels, and the timing of imaging, can influence the hepatic

SUVmean [17, 18]. The stability of hepatic ^{18}F-FDG uptake observed in this study supports its role as a reference organ while evaluating the metabolic response of lymphoma to Tisagenlecleucel.

Our study has several limitations. The retrospective nature of this study may have introduced selection and confounding bias. Our analysis did not account for potential confounding factors such as concurrent medications, previous treatments, and patient-specific characteristics that might affect ^{18}F-FDG uptake patterns independently of Tisagenlecleucel therapy. A significant limitation is the wide variability in the follow-up interval between baseline and post-treatment scans (range: 35-437 days, mean: 121.2±63.9 days). This heterogeneity in imaging timing reflects real-world clinical practice but may influence our ability to accurately differentiate early treatment-related inflammatory changes from longer-term metabolic responses and could affect the assessment of treatment response and toxicity patterns. Standardized imaging timepoints in future prospective studies would better characterize the temporal dynamics of metabolic changes following tisagenlecleucel therapy. Additionally, while ^{18}F-FDG PET/CT provides valuable metabolic information, it cannot definitively distinguish between inflammatory changes and residual disease activity. Our sample size, though reasonable for this specialized therapy, limits the statistical power to perform comprehensive subgroup analyses based on lymphoma subtypes or patient characteristics. Finally, the absence of long-term follow-up data restricts our ability to correlate early metabolic responses with definitive clinical outcomes such as overall survival and progression-free survival. Future prospective studies with larger sample sizes and extended follow-up would help address these limitations.

In conclusion, this study demonstrates that the global assessment technique using ^{18}F-FDG PET/CT can comprehensively and quantitatively evaluate metabolic changes in reticuloendothelial organs following Tisagenlecleucel therapy in DLBCL patients. Our study revealed significant reductions in the metabolic activity of lymphoma adenopathy, bone marrow, and spleen after Tisagenlecleucel therapy. These findings have important clinical implications. The significant decrease in lymphoma adenopathy metabolic activity, as measured by pvcTLG and TMTV, demonstrates the utility of ^{18}F-FDG PET/CT in quantitatively monitoring therapeutic response to Tisagenlecleucel, which may aid in early identification of responders versus non-responders. The observed reduction in bone marrow metabolic activity may reflect both treatment-related marrow suppression and resolution of disease involvement, which clinicians should consider when interpreting post-therapy imaging and managing potential hematologic complications. Similarly, decreased splenic metabolic activity in our cohort, assessed at an average of 121 days post-therapy, may indicate resolution of therapy-related immune activation and disease-related inflammation, though the clinical significance requires careful interpretation in the context of disease involvement and timing of assessment. Importantly, the preserved stability of hepatic metabolism after therapy underscores the liver's utility as a reliable reference organ while evaluating treatment response. Together, these findings suggest that tisagenlecleucel induces a broad systemic metabolic response within the reticuloendothelial system, and comprehensive assessment of multiple organs beyond tumor sites may provide valuable information for therapeutic monitoring and management of patients undergoing CAR-T cell therapy.

The authors declare that they have no conflicts of interest.

Bibliography

1. Schuster SJ, Bishop MR, Tam CS et al. Tisagenlecleucel in Adult Relapsed or Refractory Diffuse Large B-Cell Lymphoma. *N Engl J Med* 2019; 380: 45-56.
2. Davila ML, Brentjens R, Wang X et al. How do CARs work?: Early insights from recent clinical studies targeting CD19. *Oncoimmunology* 2012; 1: 1577-83.
3. El-Galaly TC, Villa D, Gormsen LC et al. ^{18}F-FDG-PET/CT in the management of lymphomas: current status and future directions. *J Intern Med* 2018; 284: 358-76.
4. Glennan P, Shehu V, Singh SB et al. PET Imaging in Chimeric Antigen Receptor T-Cell Trafficking. *PET Clin* 2024; 19: 569-76.
5. Singh SB, Bhandari S, Siwakoti S et al. PET/CT in the Evaluation of CAR-T Cell Immunotherapy in Hematological Malignancies. *Mol Imaging* 2024; 23: 15353508241257924.
6. Carr R, Barrington SF, Madan B et al. Detection of lymphoma in bone marrow by whole-body positron emission tomography. *Blood* 1998; 91: 3340-6.
7. Derlin T, Schultze-Florey C, Werner RA et al. ^{18}F-FDG PET/CT of off-target lymphoid organs in CD19-targeting chimeric antigen receptor T-cell therapy for relapsed or refractory diffuse large B-cell lymphoma. *Ann Nucl Med* 2021; 35: 132-8.
8. Beck M, Blumenberg V, Bucklein VL et al. Liver-FDG-uptake augments early PET/CT prognostic value for CD19-targeted CAR-T cell therapy in diffuse large B cell lymphoma. *EJNMMI Res* 2025; 15: 25.
9. Georgi TW, Kurch L, Franke GN et al. Prognostic value of baseline and early response ^{18}F-FDG-PET/CT in patients with refractory and relapsed aggressive B-cell lymphoma undergoing CAR-T cell therapy. *J Cancer Res Clin Oncol* 2023; 149: 6131-8.
10. Galli E, Guarneri A, Sora F et al. Baseline Tumor Burden Assessed With AI-Guided PET/CT Total Metabolic Tumor Volume (TMTV) and LDH Levels Predict Efficacy of CAR-T in Aggressive B-Cell Lymphoma. *Hematol Oncol* 2025; 43: e70029.
11. Farolfi A, Casadei B, Malizia C et al. Semiquantitative PET Parameters Refine Prognosis in CAR T-Treated Lymphoma After 1 and 3 Months: A Prospective Single-Center Study. *J Nucl Med* 2025; 66: 1183-91.
12. Kenkel TJ, Sridhar N, Hammons LR et al. Bone Marrow Aplasia after CAR-T-Cell Therapy for Relapsed/Refractory Burkitt's Lymphoma. *Med Sci (Basel)* 2023; 11: 67.
13. Yeung CCS, Woolston DW, Wu V et al. Abnormal bone marrow findings in patients following treatment with chimeric antigen receptor-T cell therapy. *Eur J Haematol* 2024; 112: 111-21.
14. Cheson BD, Fisher RI, Barrington SF et al. Recommendations for initial evaluation, staging, and response assessment of Hodgkin and non-Hodgkin lymphoma: the Lugano classification. *J Clin Oncol* 2014; 32: 3059-68.
15. Tamayo P, Martin A, Diaz L et al. ^{18}F-FDG PET/CT in the clinical management of patients with lymphoma. *Rev Esp Med Nucl Imagen Mol* 2017; 36: 312-21.
16. Paquet N, Albert A, Foidart J, Hustinx R. Within-patient variability of ^{18}F-FDG: standardized uptake values in normal tissues. *J Nucl Med* 2004; 45: 784-8.
17. Ramadori G, Cameron S. Effects of systemic chemotherapy on the liver. *Ann Hepatol* 2010; 9: 133-43.
18. Ben-Yakov G, Alao H, Haydek JP et al. Development of Hepatic Steatosis After Chemotherapy for Non-Hodgkin Lymphoma. *Hepatol Commun* 2019; 3: 220-6.